

On the nature of the intermittent pulsar PSR B1931+24

N. Rea^{1,2}, M. Kramer³, L. Stella⁴, P.G. Jonker^{2,5}, C.G. Bassa^{2,6}, P.J. Groot⁶,
G.L. Israel⁴, M. Méndez⁷, A. Possenti⁸, A. Lyne³

¹ *University of Amsterdam, Astronomical Institute “Anton Pannekoek”, Kruislaan 403, 1098 SJ, Amsterdam, The Netherlands*

² *SRON Netherlands Institute for Space Research, Sorbonnelaan 2, 3584 CA, Utrecht, The Netherlands*

³ *Jodrell Bank Centre for Astrophysics, University of Manchester, Alan Turing Building, M13 9PL, Manchester, UK*

⁴ *INAF–Astronomical Observatory of Rome, via Frascati 33, 00040, Monteporzio Catone (RM), Italy*

⁵ *Harvard-Smithsonian Center for Astrophysics, 60 Garden Street, Cambridge, MA 02138, USA*

⁶ *Department of Astrophysics, Radboud University Nijmegen, PO Box 9010, NL-6500 GL Nijmegen, The Netherlands*

⁷ *Kapteyn Astronomical Institute, Groningen University, 9700 AV, Groningen, The Netherlands*

⁸ *INAF–Astronomical Observatory of Cagliari, Poggio dei Pini, Strada 54, 09012 Capoterra (CA), Italy*

5 October 2018

ABSTRACT

PSR B1931+24 is the first intermittent radio pulsar discovered to date, characterized by a 0.8 s pulsation which turns on and off quasi-periodically every ~ 35 days, with a duty cycle of $\sim 10\%$. We present here X-ray and optical observations of PSR B1931+24 performed with the *Chandra X-ray Observatory* and *Isaac Newton Telescope*, respectively. Simultaneous monitoring from the *Jodrell Bank Observatory* showed that this intermittent pulsar was in the radio-on phase during our observations. We do not find any X-ray or optical counterpart to PSR B1931+24, translating into an upper limit of $\sim 2 \times 10^{31} \text{ erg s}^{-1}$ on the X-ray luminosity, and of $g' > 22.6$ on the optical magnitude. If the pulsar is isolated, these limits cannot constrain the dim X-ray and optical emission expected for a pulsar of that age (~ 1.6 Myr). We discuss the possibility that the quasi-periodic intermittent behavior of PSR B1931+24 is due to the presence of a low mass companion star or gaseous planet, tight with the pulsar in an eccentric orbit. In order to constrain the parameters of this putative binary system we re-analysed the pulsar radio timing residuals and we found that (if indeed hosted in a binary system), PSR B1931+24 should have a very low mass companion and an orbit of low inclination.

Key words: stars: pulsars: general — pulsar: individual: PSR B1931+24

1 INTRODUCTION

A long term radio monitoring study of the ~ 813 ms radio pulsar PSR B1931+24 (Stokes et al. 1985; Hobbs et al. 2004), revealed the peculiar intermittent behavior of this pulsar (Kramer et al. 2006). PSR B1931+24 is (so far) a unique system: it shows an active radio emission phase lasting between 5–10 days (radio-on phase, hereafter), which suddenly (in less than 10 s) switches off, and the pulsar remains undetectable for the following 25–35 days (radio-off phase, hereafter). This pattern repeats quasi-periodically, and has been monitored for the past 7 years (Kramer et al. 2006). Another peculiar property of PSR B1931+24 is its spin-down behavior. Remarkably, the pulsar rotation slows down considerably faster (by about 50%) when the pulsar is in the radio-on phase, with a frequency derivative changing from $\dot{\nu}_{\text{on}} = -(16.30 \pm 0.04) \times 10^{-15} \text{ s}^{-2}$ to $\dot{\nu}_{\text{off}} = -(10.80 \pm 0.02) \times 10^{-15} \text{ s}^{-2}$ across the two phases.

From the radio observations, typical pulsar character-

istics were derived (see Tab. 1 in Kramer et al. 2006): an estimate of the dipolar magnetic field ($B \sim 2.6 \times 10^{12} \text{ G}$), the characteristic age ($\tau_c \sim 1.6$ Myr), and the dispersion measure ($DM = 106.03 \pm 0.06 \text{ cm}^{-3} \text{ pc}$). The latter gave a rough estimate of the pulsar distance of ~ 4.6 kpc using the NE2001 model for the free electron distribution in the Galaxy (Cordes & Lazio 2002). Kramer et al. (2006) interpreted the peculiar spin-down properties of this pulsar in terms of a transient plasma flow in the magnetosphere, causing the quenching and re-ignition of the radio emission. In particular, an increase of the magnetospheric current flow during the radio-on phase, can provide an additional braking torque on the neutron star. From the observed variations in the pulsar spin-down, these authors showed that the pulsar magnetospheric electron density was consistent with the Goldreich-Julian density (Goldreich & Julian 1969). This interpretation can successfully explain the variable neutron star torque, but still fails to explain what causes the changes

in the magnetospheric plasma flow, especially if in a quasi-periodic fashion. To date, this periodicity of the radio-on and radio-off recurrence is difficult to explain in any scenario considering an isolated pulsar. As Kramer et al. (2006) pointed out, the short shut-off time of less than 10 seconds, and the rather stable pulse profile, rule out possible scenarios like precession of the neutron star. On the other hand, the long radio-off phase is in contrast with the typical nulling timescales of radio pulsars, exceeding it by almost five orders of magnitude.

Cordes & Shannon (2006) studied the possibility that PSR B1931+24 might be in a binary system with a large asteroid, surrounded by a disk of small asteroids, moving in a ~ 40 day eccentric orbit around the pulsar. This scenario suggests that the interaction between the pulsar magnetosphere and the asteroids can be responsible both for the torque change and the intermittent radio activity of PSR B1931+24. Recently, Zhang, Gil & Dyks (2007) have proposed that intermittent pulsars are old isolated neutron stars which entered (or are about to enter) the so called “death valley” (Chen & Ruderman 1993), where the polar cap voltage of the pulsar is not sufficient to power the pair production process. However, this scenario still fails to account for the quasi-periodic pulsed emission of PSR B1931+24.

Here we report on X-ray (§2) and optical (§3) observations of PSR B1931+24 taken with the *Chandra X-ray Observatory* and the *Isaac Newton Telescope*. Furthermore, in §4 we derive constraints on possible orbital parameters and companion mass by studying the radio timing residuals. In §5 and §6, we discuss our results and investigate in detail the possibility that PSR B1931+24 resides in a binary system with a ~ 35 day orbital period and a low mass companion star or a planet.

2 X-RAY OBSERVATION

The *Chandra* Advanced CCD Imaging Spectrometer (ACIS) observed PSR B1931+24 on 2006 July 20th, for an on-source exposure time of ~ 9.7 ks. The target position was placed in the standard back-illuminated ACIS S3 aimpoint, using the FAINT mode. We corrected the astrometry for any processing offset and we cleaned the image for hot pixels. Running CIAO `celldetect` and `wavedetect` tools¹, no X-ray sources were detected in the whole ACIS-S3 CCD, while four (unrelated) sources were detected in the other CCDs at $> 5\sigma$ confidence level over the background. In particular, no photons were detected in a $1''$ radius around the PSR B1931+24 radio position (see Tab.1 for the RA and DEC). We then obtained a 99% upper limit on the source count rate of 4.74×10^{-4} count s^{-1} (Gehrels 1986).

Assuming a conservative absorption value of $N_H = 8.3 \times 10^{21} \text{ cm}^{-2}$ (derived for the pulsar position from Dickey & Lockman 1990, hence considering the whole Galactic N_H in that direction), and using the PIMMS calculator², we derived a 99% upper limit on the 0.3–10 keV unabsorbed flux of $7 \times 10^{-15} \text{ erg s}^{-1} \text{ cm}^{-2}$ or $1.2 \times 10^{-14} \text{ erg s}^{-1} \text{ cm}^{-2}$, assuming a black body ($kT = 0.3 \text{ keV}$) or a power law ($\Gamma = 2.5$)

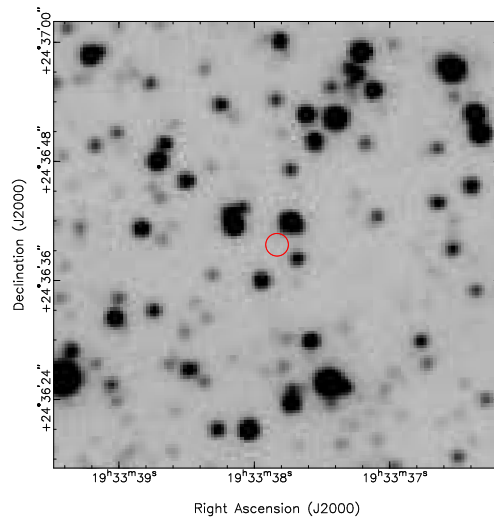


Figure 1. Finding-chart of the i' field of PSR B1931+24. The circle is the uncertainty in the pulsar position as derived from radio timing (see Tab 1).

spectral decomposition, respectively. At 4.6 kpc these fluxes translate into a 99% upper limit on the 0.3–10 keV X-ray luminosity of $1.7 \times 10^{31} \text{ erg s}^{-1}$ and $3 \times 10^{31} \text{ erg s}^{-1}$, depending on the assumed X-ray spectrum. However, note that the distance of 4.6 kpc, as inferred from the pulsar DM (Kramer et al. 2006) might well have an uncertainty of a factor of 2 due to a $\sim 30\%$ uncertainty in the Galactic electron density model (Cordes & Lazio 2002). Hence, more conservative upper limits on the luminosity would be 4 times larger than reported above.

3 OPTICAL OBSERVATIONS

We observed the field of PSR B1931+24 with the *Isaac Newton Telescope* located at the Roque de Los Muchachos Observatory in La Palma, for an exposure time of 10 minutes in three optical filters: g' , r' and i' (see Fig. 1 for the finding-chart). No optical counterpart was detected within the radio pulsar position. We derived 5σ upper limits on the optical emission of PSR B1931+24 of $g' > 22.6$, $r' > 22.4$ and $i' > 22.2$ magnitudes. We inferred these optical upper limits from the magnitudes of the faintest object detected at 5σ confidence level in the same CCD as the pulsar position. For the astrometry we used an $11' \times 11'$ subsection of the g' image where we found 85 stars from the USNO CCD Astrograph Catalogue (UCAC2; Zacharias et al. 2004). We obtained an astrometric solution, fitting the zero-point position, scale and position angle; the final rms residuals were $0''.13$ in both in RA and DEC.

We inferred the reddening in the direction of PSR B1931+24 from the N_H , which gave an $A_V = 4.64$ (Predehl & Schmitt 1995). We then converted this value into an estimate of the reddening in the filter we actually used (Rieke & Lebofsky 1985; Schlegel et al. 1998): $A_{g'} = 4.94$, $A_{r'} = 3.68$ and $A_{i'} = 2.83$. Considering a distance of 4.6 kpc, we inferred upper limits on the source absolute magnitude $i' > 4.35$, $r' > 5.2$ and $g' > 6.1$. From our upper lim-

¹ for details refer to <http://asc.harvard.edu/ciao/>

² for details refer to <http://heasarc.gsfc.nasa.gov/Tools/w3pimms.html> of: $g' > 4.35$, $r' > 5.2$ and $i' > 6.1$. From our upper lim-

Parameter	Value
RA (J2000)	19:33:37.88(5)
DEC (J2000)	24:36:40(1.5)
Epoch	52281.296676
ν (Hz)	1.22896706877(3)
$\dot{\nu}$ (10^{-15} s $^{-2}$)	-12.1501(4)
$\ddot{\nu}$ (10^{-25} s $^{-3}$)	-2.0(2)
DM (cm $^{-3}$ pc)	106.03(6)

Table 1. Parameters derived from the radio timing analysis described in §4. Errors are at 1σ confidence level.

its of the absolute optical magnitudes, we could derive a rough range of stellar types for a putative counterpart. From $r' > 5.2$, which was the most constraining limit, we could exclude all giant and super-giant stars, and deriving a spectral type later than a G8 star. Note that having we assumed the absorption value of the whole Galactic N_H : any (more realistic) lower N_H values would result in stellar types much later than a G8.

4 LIMITS ON THE ORBITAL PARAMETERS FROM THE RADIO TIMING

If PSR B1931+24 happens to be in a binary system (e.g. as investigated in detail in §5), the motion of the pulsar around the system's centre of mass should leave a periodic signature in the remaining timing residuals. We searched for this signature in radio timing data spanning almost 7 years (Kramer et al. 2006). We fit the radio timing residuals with one spin frequency derivative and a second derivative (values are reported in Tab. 1). The latter was used to remove a cubic term due to long term timing noise. In order to improve the position information, we removed the remaining timing noise by using the fit-wave method described by Hobbs et al. (2004), with a minimum period of 2 years. The pre-fit-wave residuals were then analysed for periodicities caused by low-mass companions (with masses smaller than the pulsar mass, $M_c \ll M_p$), as described by Freire et al. (2003). As Fig. 2 shows, we detected, unsurprisingly, a faint signal at a period of ~ 37 days. However, we believe this signal is consistent with a periodicity caused by the sampling of time-of-arrivals forced upon us by the quasi-periodic on-phases of the pulsar. We do not detect any other significant signal.

For a more general companion mass we also performed the following analysis of the timing residuals. The peak-to-peak amplitude of the remaining timing residuals was $\Delta t_{\text{res}} \sim 2$ ms. From this we placed limits on the corresponding orbital parameters by interpreting Δt_{res} as caused by a “Roemer delay”, i.e. the light-travel time across the orbit (e.g. Lorimer & Kramer 2005). We then set:

$$\Delta t_{\text{Roemer}} = x \left[(\cos E - e) \sin \omega + \sin E \sqrt{1 - e^2} \cos \omega \right]$$

equal to Δt_{res} . Here, E is the eccentric anomaly, e the eccentricity and ω the longitude of the periastron. Furthermore, $x = a_p \sin i/c$ is the projected semi-major axis measured in

light-seconds, which is a function of $a_p = a_R M_c/(M_p + M_c)$, the semi-major axis of the orbit³.

On the other hand, the relative orbit a_R , the orbital period and masses are related according to Kepler's 3rd law:

$$\frac{4\pi^2}{P_{\text{orb}}^2} \left(\frac{a_R}{c} \right)^3 = T_{\odot} (M_p + M_c),$$

with the masses measured in solar units and $T_{\odot} = GM_{\odot}/c^3 = 4.925490947 \mu\text{s}$. Assuming $P_{\text{orb}} \sim 35$ days and $M_p \sim 1.4M_{\odot}$ we could derive an estimate for the orbital inclination angle as a function of the companion mass in the following way: for a given companion mass M_c we performed Monte-Carlo simulations drawing possible values for E , ω and e from uniform distributions over $[0, 2\pi]$ and $[0, 1]$, respectively. Note that the distribution for the eccentricity is not expected to be uniform (i.e. it is likely to be skewed to small eccentricities) but for our purposes this assumption is sufficient as we were mostly interested in upper bounds for the inclination angle. For each companion mass, one million Monte-Carlo runs were performed and the median and 95% confidence limits were computed (see Fig. 3: the grey shadowed region is the allowed region at 95% confidence level). Hence, for reasonable companion masses the tight limit on a detectable periodicity in the timing residuals implies rather small orbital inclination angles (see also §6).

5 INVESTIGATING THE POSSIBLE BINARY NATURE OF PSR B1931+24

In this section we investigate the possibility that the peculiar characteristics of PSR B1931+24 can be explained by a low mass star or a gaseous planet moving in an eccentric orbit around the pulsar (see also §4). This causes a quasi-periodic intermittent behavior, as well as the change in the spin-down characteristics of the pulsar, in two different ways: 1) providing at the periastron passage the additional plasma needed in the Kramer et al. (2006) model, or 2) accreting material on the pulsar magnetosphere and causing the transition between the radio pulsar and the propeller regime (see for details Illarionov & Sunyaev 1975; Stella et al. 1986, 1994). In this section we discuss only this second possibility. The physics involved in the first possibility has been thoroughly investigated by Kramer et al. (2006), although without considering the wind of a companion as the source of the additional magnetospheric plasma during the radio-on phase (see also §6).

We define here three important PSR B1931+24 radii which will be used in the following.

The magnetospheric radius:

$$R_m = 2 \times 10^7 \dot{M}_{15}^{-2/7} B_9^{4/7} M_{1.4}^{-1/7} R_6^{12/7} \simeq 1.78 \times 10^9 \dot{M}_{15}^{-2/7} \text{ cm},$$

the corotation radius:

$$R_{\text{cor}} = 0.12 \times 10^8 M_{1.4}^{1/3} P_{10}^{2/3} \simeq 2.25 \times 10^8 \text{ cm},$$

and the light cylinder radius:

$$R_{\text{lc}} = 0.46 \times 10^8 P_{10} \simeq 3.74 \times 10^9 \text{ cm}.$$

³ i is the orbital inclination angle, c is the speed of light, and a_R is the size of the relative orbit.

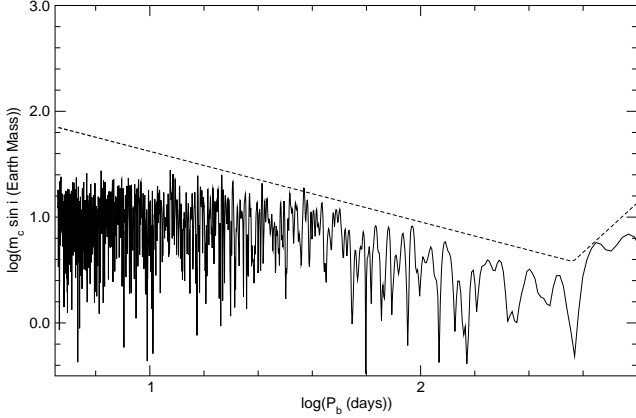


Figure 2. Lomb-Scargle spectrum of PSR B1931+24. Dashed curve indicates a 99.99% confidence level. A periodicity is detected at ~ 37 days, but see text for details.

These three radii represent, respectively: i) the balance of the gravitational force and the ram pressure of the infalling material, ii) the centrifugal barrier for the infalling material due to the pulsar rotation, and iii) the place where the pulsar magnetic field lines open such that their tangential velocity do not exceed the speed of light (Illarionov & Sunyaev 1975; Ruderman & Sutherland 1975).

We define: $B_9 = B_{\text{ns}}/10^9 \text{ G}$ is the neutron star magnetic field, P_{10} is the spin period in units of 10 ms, $\dot{M}_{15} = \dot{M}/10^{15} \text{ g s}^{-1}$ is the mass inflow rate toward the neutron star, and $M_{1.4} = M_{\text{ns}}/1.4M_{\odot}$ and $R_6 = R_{\text{ns}}/10^6 \text{ cm}$ are the mass and the radius of the neutron star, hereafter assumed $M_{1.4} = R_6 = 1$. Note that during the orbital motion, the only variable radius is $R_m \propto \dot{M}_{15}^{-2/7}$.

5.1 Radio pulsar is on

If the mass inflow rate from the putative companion star is very low, as might happen at apastron of an eccentric orbit, the magnetosphere of the neutron star might be larger than the light cylinder and corotation radii ($R_m > R_{\text{lc}} > R_{\text{cor}}$).

As a result, the centrifugal barrier is closed, which means that incoming material from the companion star is prevented from falling towards the neutron star magnetosphere or surface. In this case the neutron star might behave as a radio pulsar. The pulsar radiation pressure dominates over the ram pressure of the inflowing material, preventing the matter to penetrate towards the neutron star (Illarionov & Sunyaev 1975; Davis & Pringle 1981; Stella et al. 1994; Campana et al. 1998).

This occurs when the mass inflow rate (\dot{M}) is smaller than the limiting value:

$$\dot{M}_{15, \text{radio-off}} = 5.4 \times 10^{-2} B_9^2 P_{10}^{-7/2} M_{1.4}^{-1/2} R_6^6 \simeq 0.075,$$

above which the radio pulsations would quench, even as rapidly as ~ 10 s.

It is worth noting that when $\dot{M} \sim \dot{M}_{15, \text{radio-off}}$, the

radio pulsar emission is not in equilibrium (Illarionov & Sunyaev 1975; Shaham & Tavani 1991), depending on the stability of the mass inflow rate; sporadic variability of the radio-on duration of PSR B1931+24 might take place, as indeed observed (Kramer et al. 2006). Furthermore, during the radio-on phase, variations in the pulsar DM as a function of the orbital phase are expected. Unfortunately the observations were performed at one frequency, making impossible to put a meaningful limit on the DM variability (see also Kramer et al. 2006).

5.2 Radio pulsar is off

If the mass inflow rate starts to increase, e.g. approaching periastron, we expect a correlated decrease of the magnetospheric radius, which eventually becomes smaller than the light cylinder radius ($R_{\text{lc}} > R_m > R_{\text{cor}}$). This happens when the mass inflow rate towards the neutron star becomes larger than the limiting value $\dot{M}_{15, \text{radio-off}}$; at this point the pulsar radiation pressure is overcome by the ram pressure of the infalling material quenching the radio pulsar mechanism. Different regimes are then allowed at this stage. If R_m remains larger than R_{cor} , which means $\dot{M}_{15, \text{radio-off}} < \dot{M} < \dot{M}_{15, \text{acc}}$, with

$$\dot{M}_{15, \text{acc}} = 5.97 B_9^2 P_{10}^{-7/3} M_{1.4}^{-5/3} R_6^6 \simeq 1.4 \times 10^3,$$

then the magnetosphere of the neutron star still rotates in a super-Keplerian motion, and the inflowing material might either accumulate outside the magnetospheric boundary or be swept away by the magnetospheric drag: this is called the “propeller” regime (Pringle & Rees, 1972; Illarionov & Sunyaev 1975; Davies & Pringle 1981; Wang & Robertson 1983; Stella, White & Rosner 1986).

Given the upper limits we derived for the possible companion star (see § 3 and § 4), there is only a very small chance that the \dot{M} , due to the wind loss of the companion, overcomes $\dot{M}_{15, \text{acc}}$. We will then consider hereafter only the possibility that the radio-off phase is driven by the propeller regime, excluding the surface accretion scenario.

When the radio pulsations are quenched, the spin down behavior of the pulsar is not driven anymore by the magnetic dipolar loss as it was before. What happens to the pulsar spin-down during the propeller regime is still rather controversial, and requires detailed hydrodynamic simulations (Romanova et al. 2003). Depending on which kind of instability and shock takes place on the pulsar magnetosphere, the spin-down rate might either increase further or be reduced by the angular momentum transferred by the infalling material to the magnetosphere.

In the PSR B1931+24 case, it is clear that the infalling material should provide a certain rotational energy in order to make the pulsar slow down less efficiently during the radio-off phase, changing the spin-down of the neutron star by $\Delta\dot{\nu} = \dot{\nu}_{\text{on}} - \dot{\nu}_{\text{off}} = -5.5 \pm 0.4 \times 10^{-15} \text{ Hz s}^{-1}$, which converted in energy corresponds to $\Delta\dot{E} \simeq 4\pi^2 I \nu \Delta\dot{\nu} \simeq 2.6 \times 10^{30} \text{ erg s}^{-1}$.

When the infalling matter reaches the neutron star magnetosphere, the source is expected to emit in the X-ray band with a minimum luminosity of:

$$L_{\text{radio-off}} = 7 \times 10^{31} B_9^2 P_{10}^{-9/2} M_{1.4}^{1/2} R_6^6 \simeq 0.12 \times 10^{31} \text{ erg s}^{-1},$$

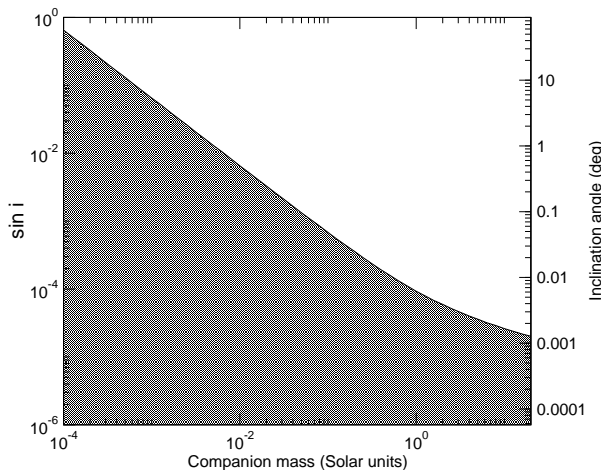


Figure 3. Limits on the orbital inclination angle as a function of the companion mass as derived from the pulsar radio timing. For each companion mass, one million Monte-Carlo runs were performed, the median and 95% confidence limits were computed. The grey shadowed region is the allowed region at 95% confidence level.

and a maximum luminosity related to the maximum wind loss we expect from the inferred companion type. For a stellar type later than a G8, we expect the X-ray luminosity of the system in the radio-off phase to be between $1.2 \times 10^{30} - 1.6 \times 10^{32} \text{ erg s}^{-1}$.

After the periastron passage, the low-mass companion star moves towards apastron, the magnetospheric boundary expands because of the decreasing mass inflow rate, the centrifugal barrier closes and the radio pulsar mechanism can resume again.

6 DISCUSSION

The upper limits we derived from these X-ray and optical observations of PSR B1931+24 during the radio-on phase, are not deep enough to detect the typical X-ray luminosity ($< 10^{29} \text{ erg s}^{-1}$; Becker & Trümper 1997) and optical magnitude ($V > 28$; Mignani et al. 2007) of an isolated pulsar of $\sim 1.6 \text{ Myr}$, as PSR B1931+24.

On the other hand, if the pulsar is hosted in a binary system, we derived tight constraints on the putative companion and its orbital parameters. We constrained the companion to be a low mass star later than a G8 type or a gaseous planet. For an orbital inclination of 0.1 degree the companion would have a mass $M_c < 0.01 M_\odot$, while with a smaller inclination of 0.01 degree, the companion mass is allowed to be $M_c < 0.1 M_\odot$ (all at 95% confidence level; see Fig. 3).

In the binary scenario (see § 5), the pulsar intermittence can be explained by the transition between the radio pulsar regime and the propeller regime during the orbital motion. The X-ray upper limits we derived are unfortunately rel-

ative to the radio pulsar dominated regime (note that the source was radio-on during the observations), and not to the propeller regime when the source can be bright in the X-ray due to accretion of matter onto the pulsar magnetosphere. Our *Chandra* observation was in fact aimed at detecting a possible X-ray emission from PSR B1931+24 during its radio-off phase. Unfortunately, the relatively uncertain duration of both phases (the radio-on phase rarely might happen to be longer than the average duration), and the relatively large error (\sim a few days) on the putative periastron passage, made the observation be performed during the radio-on phase of the pulsar.

Note that the insufficient flux detection limit of current and past X-ray surveys and monitoring programs (e.g. ROSAT and the RXTE/ASM), do not make the non detection of an X-ray counterpart in previous X-ray surveys at all constraining.

Although very successful in explaining the intermittence, the quasi-periodicity and the torque variations of PSR B1931+24, this binary scenario still presents several unsolved issues. One issue of this scenario, and to some extent also to the “asteroid” model (Cordes & Shannon 2006), is the very small orbital inclinations required by the radio timing studies (§ 4 and Fig. 3). For a random distribution of inclination angles, the probability of observing a system at an angle less than a value i_0 , is $p(i < i_0) = 1 - \cos i_0$. Considering the favorable case of an angle of 15° (a gaseous planet; see Fig. 3), the probability of observing such a system is $p(i < 15^\circ) = 3.4\%$. A chance of 3.4% is not very high, although still worth to be considered.

Another issue concerns the accretion rate from the companion. Can the accretion from the low wind loss of such a small mass star or gaseous planet be high enough to switch the pulsar from the radio emitting regime to the propeller regime? Typical wind rates for e.g. a K0 star are insufficient to produce the limiting value of $\dot{M}_{15, \text{radio-off}}$ by ~ 2 orders of magnitude. This problem might be partially (but not totally) alleviated by taking into account the irradiation process (Podsiadlowski 1991; D’Antona & Ergma 1993). In particular, a low mass star irradiated by the radio pulsar is expected to expand even if the radiation bath is not particularly extreme, and the wind of the star to increase substantially. However, the irradiation process cannot be dominant on the stellar wind from a G8 to K0 star, mainly because of the relatively low rotational energy of PSR B1931+24 with respect to the surface temperature of the companion star ($L_{\text{irr}} = f \dot{E}_{\text{rot}} (R_s/2a_p)^2$, where R_s is the companion star radius). For lower mass stars or considering a gaseous planet orbiting around the pulsar, this process might have instead a substantial role, and might produce strong winds towards the pulsar while at periastron.

If the weak stellar wind from the low-mass companion star is insufficient to drive the radio pulsar in the propeller regime, it is instead strong enough to provide the amount of plasma needed to produce the spin-down change in the scenario proposed by Kramer et al. (2006). Note that in this picture, at the periastron passage we expect the radio-on phase, while in the propeller scenario it is expected at the apastron of the orbit. However, while the propeller scenario naturally explains the quenching of the radio emission, in this picture the radio quenching still remains puzzling: we

would in fact expect to see the pulsar at all the time, although with two different spin-down behavior.

ACKNOWLEDGMENTS

We acknowledge the director of the Chandra X-ray Observatory, Harvey Tananbaum, for promptly according us an observation of PSR B1931+24 through his Director Discretionary Time, and for useful comments on this draft. We also thank the Chandra team for the efficiency during the scheduling process. We are grateful to the referee, S. Ransom, for his valuable suggestions which largely improved our work. NR acknowledges support from an NWO Veni Fellowship and thanks F. Verbunt, M. Burgay, D. Russell, and the ATNF-Epping pulsar group, for useful comments and discussions.

REFERENCES

- Becker, W., Trümper, J. 1997, *A&A*, 326, 682
 Campana, S., Colpi, M., Mereghetti, S., Stella, L., Tavani, M. 1998, *A&ARv*, 8, 279
 Cordes, J. M. & Lazio, J. T. W. 2002, preprint (astro-ph/0207156)
 Cordes, J. M. & Shannon, R. M. 2006, *ApJ* submitted, astro-ph/0605145
 D’Antona, F. & Ergma, E. 1993, *A&A* 269, 219
 Dickey, J. M. & Lockman, F. J. 1990, *ARA&A*, 28, 215
 Freire, P. C., Camilo, F., Kramer, M., Lorimer, D. R., Lyne, A. G., Manchester, R. N., D’Amico, N. 2003, *MNRAS* 340, 1359
 Gehrels, N. 1986, *ApJ*, 303, 336
 Goldreich, P. & Julian, W. H. 1969, *ApJ*, 157, 869
 Hobbs, G., Lyne, A. G., Kramer, M., Martin, C. E., Jordan, C. 2004, *MNRAS*, 353, 1311
 Illarionov, A. F. & Sunyaev, R. A. 1975, *A&A*, 39, 185
 Kramer, M., Lyne, A. G., O’Brien, J. T., Jordan, C. A., Lorimer, D. R. 2006, *Science*, 312, 549
 Lorimer, D. & Kramer, M., 2005, *Handbook of pulsar astronomy*, Cambridge University Press
 Mignani, R. P., Bagnulo, S., De Luca, A., et al. 2007, *A&SS*, in press, astro-ph/0608025
 Podsiadlowski, P. 1991, *Nature*, 350, 136
 Predehl, P. & Schmitt, J. H. 1995, *A&A*, 293, 889
 Rieke, G. H & Lebofsky, M. J. 1985, *ApJ*, 288, 618
 Romanova, M. M., Toropina, O. D., Toropin, Yu. M., Lovelace, R. V. 2003, *ApJ*, 588, 400
 Ruderman, M. A. & Sutherland, P. G. 1975, *ApJ*, 196, 51
 Chen, K. & Ruderman, M. 1993, *ApJ*, 402, 264
 Schlegel, D. J., Finkbeiner, D. P. & Davis, M. 1998, *AJ*, 115, 525
 Shaham, J. & Tavani, M. 1991, *ApJ*, 377, 588
 Stella, L., White, N. E. & Rosner, R. 1986, *ApJ*, 308, 669
 Stella, L., Campana, S., Colpi, M., Mereghetti, S., Tavani, M. 1994, *ApJ*, 423, L47
 Stokes, G. H, Taylor, J. H., Weisberg, J. M., Dewey, R. J. 1985, *Nature* 317, 787
 Yakovlev, D. G. & Pethick, C. J. 2004, *ARA&A*, 42, 169
 Zacharias, N., Urban, S. E., Zacharias, M. I., Wycoff, G. L.,

Hall, D. M., Monet, D. G., Rafferty, T. J 2004, *AJ*, 127, 3043

Zhang, B., Gil, J. & Dyks, J. 2007, *MNRAS*, 374, 1103

Zavlin, V.E. & Pavlov, G.G. 2004, *ApJ*, 616, 452